International Journal of Computing and Digital Systems
ISSN (2210-142X)
Int. J. Com. Dig. Sys. 10, No.1 (Aug-2021)

http://dx.doi.org/10.12785/ijcds/100172

Image Denoising Based on Statistical Nearest Neighbor and Wave Atom Transform

Akula Suneetha[1] and Edara Srinivasa Reddy[2]

[1] KKR & KSR Institute of Technology and Sciences, Department of CSE, Guntur, Andhra Pradesh, India.
[2]University College of Engineering & Technology, Acharya Nagarjuna University, Department of CSE, Nagarjuna Nagar, Guntur, Andhra Pradesh, India.

Received 9 October. 2020, Revised 27 March. 2021, Accepted 3 April. 2021, Published 5 Aug. 2021

Abstract: In this research, a hybrid multiresolution method is proposed for image denoising, which is the combination of Statistical Nearest Neighbor (SNN) and Wave Atom Transform (WAT) approaches. The proposed model captures both patterns across oscillation and coherence of the pattern along with the oscillations. In this research, KODAK database is utilized for analyzing the proposed model performance, where the acquired color images are contaminated with Gaussian noise of σϵ [5,10,15,20,25,35,40 and 50] and noise range (0, 0.1, 0.35, 0.65, 0.8. 0.9, and 1.0). The denoising performance of the SNN-WAT model is analyzed by means of Gradient Magnitude Similarity Deviation (GMSD), Feature Similarity Index (FSIM), FSIM with chromatic information ($FSIM_C$), Structural Similarity Index (SSIM), Mean SSIM index (MSSIM) and Peak Signal-to-Noise Ratio (PSNR). In the experimental phase, proposed SNN-WAT model averagely enhanced maximum of 4 dB and minimum of 0.1 dB of PSNR compared to the existing models like Non-Local-Means (NLM) with SNN technique.

Keywords: Gaussian Noise, Hard Thresholding, Image Denoising, Statistical Nearest Neighbor, Wave Atom Transform

1. Introduction

Generally, the digital images are corrupted by noise artifacts like salt and pepper noise, Gaussian noise, Quantization noise, etc., due to image transmission, compression and acquisition [1]. In image denoising, most of the color and gray scale images are corrupted with Gaussian noise because of higher temperature in electronic circuit and poor illumination. Thus, the images with Gaussian noise are utilized as the benchmark images for assessing image denoising algorithms performance [2]. Usually, the image degradation significantly affects the process of edge detection, feature recognition, segmentation, etc. Hence, the restoration techniques are used to correct the interpretation of the images [3]. The main purpose of denoising is for enhancing the visual quality of the images and preserve the complex structures and image details like texture and edges [4-5]. The digital image denoising contains two kinds of methods such as spatial filtering techniques and transform domain processing techniques [6]. In recent decades, numerous non-linear filtering techniques are used for image denoising, where each filtering technique has its own limitations. Wiener filter is a statistical technique that has complex computation and relatively expensive. Therefore, wiener filter needs an accurate noise model, otherwise it is hard to apply in real time digital images [7]. The non-local means filtering technique do not blur the image edges that are considered as a major concern. Another disadvantage in this filtering technique is that it estimates only grey level values that are not robust to attain better denoising performance [8-9].

Additionally, bilateral filter does spatial averaging without smoothing the image edges [10]. Hence, the above mentioned filtering techniques attained better performance in image denoising, still it is not proven reliable for image denoising, because of few factors such as lighting variations, illuminations, etc. Thus, the transform domain processing techniques gained more popularity, but an individual transform technique does not describe the local information and features of the digital images. For enhancing the ability of image denoising, a hybrid SNN-WAT model is developed in this article. The contribution of this research work is given below.

E-mail address: sunitha_akula1@yahoo.co.in, edara67@yahoo.com

- SNN technique significantly decreases the error of noise patches that deblur the lower contrast image regions.
- WAT with hard thresholding captures both patterns across oscillation and coherence of the pattern along with the oscillations for better detection of noisy pixels. Also, it adjusts the anisotropic patterns and local direction patterns of the images that preserves and smooths the image edge details. The combined SNN-WAT model preserves the edges in high gradient region of the digital images and delivers good approximate scene illumination related to the existing models like NLM-SNN, Fast and Flexible Denoising convolutional neural network (FFDNet), Attention-guided Denoising convolutional neural network (ADNet) and ADNet-B. In the experimental phase, the proposed SNN-WAT model achieved better denoising performance compared to the existing models on KODAK dataset by means of PSNR, SSIM, MSSIM, FSIM, $FSIM_c$ and GMSD.

Some of the existing papers in image denoising are reviewed in Section 2. Section 3 details about dataset collection and undertaken methodologies with mathematical expressions. Simulation result of the proposed model is briefly detailed in Section 4. Meanwhile, the conclusion of the work is given in Section 5.

2. Literature review

L. Fan et al. [11] impl7emented a new adaptive boosting methodology to improve low rank based image denoising. In this literature paper, the signal was strengthened by combining boosting methodology with the dynamic parameters and also by leveraging the prior denoised image. Then, the boosting methodology was correlated with weighted nuclear norm minimization technique, whose feasibility was proven theoretically. Therefore, the dynamic boosting parameters were pre-determined by an optimal analysis in every iteration of the boosting methodology. Additionally, an adaptive patch search approach was utilized for achieving similar patches. Further, correlation coefficient was employed for determining the optimal iteration number. Experimental outcome shows that the developed methodology preserves more information, while removing noise and also outperforms several existing denoising approaches in light of PSNR and SSIM. Y. Zhang et al. [12] presented an effective methodology for image denoising namely Least Squares Support Vector Regression (LSSVR). The conventional LSSVR method omits sampling distribution that degrades image denoising performance. In this research, a fuzzy density based SVR approach was developed for an effective image denoising. Initially, the developed methodology allocates fuzzy priority to each and every sample on the basis of density weight. Here, the fuzzy density weight was generated for estimating the joint probability density function using neighborhood and pixel density functions. The extensive experimental outcome shows that the fuzzy density based SVR approach was superior compared to the existing denoising techniques. In contrast to this, the developed methodologies were not much efficient for deblurring process, due to high expensive computation.

G. Wang et al. [13] implemented a novel fuzzy decision filter for image denoising. The developed filter utilizes fuzzy membership value for describing the pixel property and differentiating the noise free and noisy image pixels. The pixel values keep unchanged if the central pixel value was noise free. Or else, the pixel values were replaced by un-corrupted pixel values. Simulation outcomes showed that the developed fuzzy decision filter has better performance than the popular existing filtering techniques. Though, the developed filter usually wipes small features that significantly degrades the performance. Additionally, J.J.J. Babu and G.F. Sudha, [14] developed an adaptive fuzzy logic approach for speckle denoising. Initially, fuzzy logic was employed on the variation coefficients of noisy images and then a suitable filter was adaptively selected for improving noise suppression and preserving image details. Next, a weight averaging filter was used for distinguishing the image edges and noise. In this research, SSIM was utilized as a tuning parameter that depends on the quantity of noise present in the image. Experimental investigation shows that the developed method has significant noise suppression and also effectively preserves the structural details and image edges compared to the existing methodologies. While performing experiments with two level process, the system computational complexity was bit high. V.P. Ananthi and P. Balasubramaniam [15] developed a new impulse noise detection methodology on the basis of fuzzy sets. Generally, the Interval Valued Intuitionistic Fuzzy Sets (IVIFSs) were combined with type 2 linguistic uncertainty, where the interval width was indicated as vagueness. The developed methodology performs image denoising by considering the vagueness as entropy value. In this scenario, the IVIFSs were generated by diminishing the entropy value and by considering the probabilistic sum of the membership interval. Finally, directional kernels and fuzzy filter were employed to detect the image noise pixels. The comparative investigation shows that the developed methodology performs well related to the existing filtering techniques. H.R. Shahdoosti and S.M. Hazavei, [16] developed a methodology for image denoising on the basis of redundant and sparse dictionaries. At first, a hard thresholding operator was utilized to guarantee the similarity between noisy and denoised images and also to deliver noise free image. Next, a matching algorithm was developed to represent the dictionary elements, and then a sparse vector was utilized for all the patches in a group. Simulation consequences show that the developed method attained better performance in denoising the images, which were contaminated with Gaussian noise compared to the existing methods. However, the developed methodologies have the issue of sparse matrices, where it needs more memory and time for image denoising.

M. Rakhshanfar and M.A. Amer [17] constructed an effective image denoiser by employing dissimilar image Gaussian noise filters. In this study, the filters were combined utilizing dissimilar cascaded forms that provide a high quality output than the individual one. Simulation outcome showed that the developed multi-domain denoiser obtained significant performance in denoising than its building blocks. In addition, the developed multi-domain denoiser was combined with the existing denoisers for developing a superior denoiser, when adding imperceptible complexity. The multi-domain denoiser denotes several pixels in spatial positions that may results in artifacts which was considered as a major concern. Additionally, B. Jin et al. [18] developed bilateral filter with gradient histogram preservation approach for removing noise from the digital images and preserving the image edges with low noise amplification. The experimental consequence showed that the developed denoising techniques delivers higher PSNR value than the conventional techniques. The bilateral filter was a statistical approach that was relatively expensive and complex computation. Though, bilateral filter requires an accurate noise model, or else it was very difficult to apply in real time images. Further, I. Frosio and J. Kautz, [19] developed NLM-SNN technique for image denoising, where the developed technique outperforms the conventional NN in the case of colored and white noise. Generally, higher SNN was required for generating the images with superior quality that may lead to system complexity. V.P. Ananthi and P. Balasubramaniam [15] developed a new impulse noise detection methodology on the basis of fuzzy sets. Generally, the Interval Valued Intuitionistic Fuzzy Sets (IVIFSs) were combined with type 2 linguistic uncertainty, where the interval width was indicated as vagueness. The developed methodology performs image denoising by considering the vagueness as entropy value. In this scenario, the IVIFSs were generated by diminishing the entropy value and by considering the probabilistic sum of the membership interval. Finally, directional kernels and fuzzy filter were employed to detect the image noise pixels. The comparative investigation shows that the developed methodology performs well related to the existing filtering techniques. H.R. Shahdoosti and S.M. Hazavei, [16] developed a methodology for image denoising on the basis of redundant and sparse dictionaries. At first, a hard thresholding operator was utilized to guarantee the similarity between noisy and denoised images and also to deliver noise free image. Next, a matching algorithm was developed to represent the dictionary elements, and then a sparse vector was utilized for all the patches in a group. Simulation consequences show that the developed method attained better performance in denoising the images, which were contaminated with Gaussian noise compared to the existing methods. However, the developed methodologies have the issue of sparse matrices, where it needs more memory and time for image denoising.

M. Rakhshanfar and M.A. Amer [17] constructed an effective image denoiser by employing dissimilar image Gaussian noise filters. In this study, the filters were combined utilizing dissimilar cascaded forms that provide a high quality output than the individual one. Simulation outcome showed that the developed multi-domain denoiser obtained significant performance in denoising than its building blocks. In addition, the developed multi-domain denoiser was combined with the existing denoisers for developing a superior denoiser, when adding imperceptible complexity. The multi-domain denoiser denotes several pixels in spatial positions that may results in artifacts which was considered as a major concern. Additionally, B. Jin et al. [18] developed bilateral filter with gradient histogram preservation approach for removing noise from the digital images and preserving the image edges with low noise amplification. The experimental consequence showed that the developed denoising techniques delivers higher PSNR value than the conventional techniques. The bilateral filter was a statistical approach that was relatively expensive and complex computation. Though, bilateral filter requires an accurate noise model, or else it was very difficult to apply in real time images. Further, I. Frosio and J. Kautz, [19] developed NLM-SNN technique for image denoising, where the developed technique outperforms the conventional NN in the case of colored and white noise. Generally, higher SNN was required for generating the images with superior quality that may lead to system complexity.

K. Zhang et al. [26] developed FFDNet model to achieve better tradeoff between denoising performance and inference speed. The developed FFDNet model eliminates spatial variant noise with faster speed, and has the ability to manage an extensive range of noise levels, which ranges between [0, 75]. In addition, C. Tian et al. [27] developed ADNet model for image denoising that includes 4 blocks; sparse, feature enhancement, attention, and reconstruction. In sparse block common convolutions were used to eliminate the noise. In feature enhancement block, global and local features were used to improve the expressive ability of the developed model. The attention block utilized finely extracted noise information for reducing the complexity and improving the efficiency of the denoising model. Lastly, reconstruction block constructs the denoised image by using the obtained noise mapping. The effects from the shallow layers on deep layers are weakened with the growth of the network depth that results in ill-posed denoising issue. In order to address these concerns, a new model; SNN-WAT is proposed in this research paper for improving the image denoising performance, especially in case of Gaussian noise. Table I represents the overview of literature section that includes advantages, disadvantages, methodologies, etc.

TABLE I. OVERVIEW OF LITERATURE

Author	Year	Advantage	Limitation
G. Wang et al. [13]	2015	By using fuzzy membership value, the developed filter superiorly differentiates and describes the pixel property of noise free and noisy image pixels.	The developed fuzzy decision filter wipes small features, which degrades the denoising performance.
B. Jin et al. [18]	2015	The developed filter preserves the image edges with lower noise amplification.	Bilateral filter was relatively expensive and has complex computation.
Y. Zhang et al. [12]	2016	Performs effective image denoising by allocating fuzzy priority to each sample based on density weight.	Due to higher expensive computation, fuzzy density based SVR method was inefficient in deblurring process.
J. J. J. Babu, and G. F. Sudha,[14]	2016	The developed filter effectively improves the noise suppression and preserves the image structural details.	System computational complexity was bit higher in this work, while performing experiments with two level processes.
V. P. Ananthi, and P. Balasubramaniam, [15]	2016	The directional kernels and fuzzy filter effectively detects the image noise pixels.	The developed method consumes more memory and time for image denoising.
I. Frosio, and J. Kautz, [19]	2018	The developed NLM-SNN technique delivers better denoising performance in real time applications.	To generate the images with superior quality, higher SNN was required that may leads to system complexity.
K. Zhang et al. [26]	2018	The developed FFDNet model effectively eliminates spatially variant noise and also manages an extensive range of noise levels.	Over-smoothing the image details was a major issue in this study.
L. Fan et al. [11]	2019	While removing noise, the developed adaptive boosting method effectively preserves more image information.	The developed adaptive boosting method was inefficient in deblurring process, due to higher expensive computation.
H. R. Shahdoosti, and S. M. Hazavei, [16]	2019	Hard thresholding operator and block matching algorithm effectively finds the noise free image pixels to achieve better image denoising performance.	It has an issue of sparse matrices, so it consumes higher memory space and time for image denoising.
M. Rakhshanfar, and M. A. Amer, [17]	2019	By using dissimilar cascaded forms, the developed filter delivers a higher quality output.	Multi-domain denoiser has numerous image pixels in spatial positions that may results in artifact introduction.
C. Tian et al. [27]	2020	The developed method efficiently reduces the system complexity and improves the denoising performance.	Ill-posed denoising issue was a major concern in this study.

3. PROPOSED MODEL

In image processing and computer vision applications, elimination of noise from the images is a fundamental task. During image acquisition and transmission, the image quality is degraded due to numerous factors like chromatic aberration, distortion, pixel defects, uniformity, etc. So, it is compulsory to diminish noise in the images before commencing other image processing tasks [20].

A. Image collection

In this research study, the digital images are collected from the KODAK dataset for experimental analysis. The undertaken dataset is collected by the Eastman Kodak company and it contains twenty five uncompressed portable graphics format images with the size 768×512. Some of the sample images of KODAK dataset are presented in figure 1. After collecting the images, denoising is carried-out utilizing SNN with WAT.

Figure 1. Some of the sample images of KODAK dataset

B. Statistical Nearest Neighbor

Initially, consider a Gaussian noise corrupted image with variance σ^2 . Then, search for similar patches is carried out by calculating the distance among patches with similar size μ_r, but in dissimilar positions of the corrupted image, as shown in equation (1).

$$d^2\left(\mu_r,\gamma_k\right)=\left(\frac{2\sigma^2}{P}\right)\times\sum_{i=o}^{P-1}G\left(0,1\right)^2 \quad (1)$$

Where, σ^2 is represented as variance, μ is denoted as mean, $G\left(\mu\sigma^2\right)$ is represented as Gaussian random value and γ_K is indicated as neighborhood patch. Sum of squared normal value P has x_P^2 distribution, so $d^2\left(\mu_r,\gamma_k\right)\sim\left(\frac{2\sigma^2}{P}\right)\times x_P^2$ as mentioned in the equation (2).

$$E\left[d^2\left(\mu_r,\gamma_k\right)\right]=2\sigma^2 \quad (2)$$

For dealing with a tractable concern, SNN methodology is introduced that supports intuition with analytical evidence. In this scenario, a simplified toy concern is described, where the reference patch 1×1 with μ is contaminated by σ^2 with variance μ_r □ $G(\mu,\sigma^2)$, where μ_r is indicated as noisy reference patch. Therefore, the probability P and cumulative density functions ϕ are mathematically stated in the Eq. (3) and (4).

$$P\left(\mu_r<x\right)=\Phi_{\mu,\sigma^2}\left(x\right)=\frac{1}{2}\times\left[1+erf\left(\frac{x-\mu}{\sqrt{2\sigma}}\right)\right] \quad (3)$$

$$\phi_{\mu,\sigma^2}\left(x\right)=\Phi'_{\mu,\sigma^2}\left(x\right)=\frac{1}{\sqrt{2\pi\sigma}}e^{-0.5\left[\frac{(x-\mu)}{\sigma}\right]^2} \quad (4)$$

Let us assume N is a noisy neighbors $\{\gamma_k\},k=1,...N$ where N replicas of μ and it is distributed as $G\left(\mu,\sigma^2\right)$. Hence, the probability P and cumulative density functions ϕ of $\{\gamma_r\},k=1,....N$ is mathematically denoted in the Eq. (5) and (6).

$$P\left(\gamma_k<x\right)=\Phi_{mix}\left(x\right)=p_r\Phi_{\mu,\sigma^2}\left(x\right)+p_f\Phi_{\mu f,\sigma^2}\left(x\right) \quad (5)$$

$$\phi_{mix}\left(x\right)=\Phi_{mix}\left(x\right)'=p_r\phi_{\mu,\sigma^2}\left(x\right)+p_f\phi_{\mu f,\sigma^2}\left(x\right) \quad (6)$$

In addition, the simplified estimator $\mu\left(\mu_r\right)$ is defined in Eq. (7).

$$\mu\left(\mu_r\right)=\frac{1}{N_n}\sum_{k=1,...N_n}\gamma_k \quad (7)$$

Where, p_f is represented as false matches, where the distribution is $G\left(\mu_{f,}\sigma^2\right)$ and γ_k is stated as noisy neighbor patch [19]. The error prediction of $\mu\left(\mu_r\right)$ is decomposed into variance and bias terms for a reference patch μ_r and it is mathematically derived by using the Eq. (8), (9) and (10).

$$\in^2\left(\mu_r\right)=\int_\mu\left(\mu-\mu\right)^2p\left(\mu\right)d\mu=\in_{bias}^2\left(\mu_r\right)+\in_{\text{var}}^2\left(\mu_r\right) \quad (8)$$

$$\in_{bias}^2\left(\mu_r\right)=\int_\mu\left(E\left[\mu\right]-\mu\right)^2p\left(\mu\right)d\mu=\left\{E\left[\mu\left(\mu_r\right)-\mu\right]\right\}^2 \quad (9)$$

$$\in_{\text{var}}^2\left(\mu_r\right)=\int_\mu\left(\mu-E\left[\mu\right]\right)^2p\left(\mu\right)d\mu=Var\left[\mu\left(\mu_r\right)\right] \quad (10)$$

For notation clarity, eliminate the dependency of $\mu\left(\mu_r\right)$ from μ_r with-in the integrals and $p\left(\mu\right)$ is the probability density function of μ. At last, compute the total error of the estimator using the distribution of μ_r, as indicated in the Eq. (11), (12) and (13).

$$\in^2=\in_{bias}^2+\in_{\text{var}}^2 \quad (11)$$

$$\in_{bias}^2=\int_{\mu_r}\in_{bias}^2\left(\mu_r\right)\phi_{\mu,\sigma^2}\left(\mu_r\right)d\mu_r \quad (12)$$

$$\in_{\text{var}}^2=\int_{\mu_r}\in_{\text{var}}^2\left(\mu_r\right)\phi_{\mu,\sigma^2}\left(\mu_r\right)d\mu_r \quad (13)$$

The set $\{\gamma_k\},k=1...N_n$ comprises of N_n samples, while the neighbors are collected using NN methodology. In order to calculate the estimation error, the statistical distribution of $E\left[\mu\left(\mu_r\right)\right]$ and $Var\left[\mu\left(\mu_r\right)\right]$ are computed using the Eq. (9) and (10). Let us define $\delta=\left|\gamma N_n\left(\mu_r\right)-\mu_r\right|$, which is the distance of $N_n{}^{th}$ nearest neighbors from μ_r. Apart from a normalization factor ξ, every γ_k is independent of other factors. However, the probability of N_n in $\left[\mu_r-\delta,\mu_r+\delta\right]$ interval is the product of 3 terms, (i) probability of $N_n{}^{th}$ neighbor lies at distance μ_r and δ, (ii) probability of $N-N_n$ samples lies outside of the interval $\left[\mu_r-\delta,\mu_r+\delta\right]$ and (iii) probability of N_n-1 samples lies in the $\left[\mu_r-\delta,\mu_r+\delta\right]$ range. Therefore, the probability density function of $p\left(\delta\right)$ describes the probability of identifying N_n samples with the distance δ from μ_r that is defined in Eq. (14).

$$p(\delta) = \xi \times pin(\delta)^{N_n - 1} P_{bou}(\delta)\left[1 - pin(\delta)\right]^{N - N_n} \quad (14)$$

Where,

$$pin(\delta) = \Phi_{mix}(\mu_r + \delta) - \Phi_{mix}(\mu_r - \delta)$$

$$p_{bou}(\delta) = \phi_{mix}(\mu_r - \delta) - \phi_{mix}(\mu_r + \delta)$$

By forcing $\int_0^{+\infty} p(\delta)\, d\delta = 1$, the normalization factor ξ is identified. Using Eq. (14), expected value and $E\left[\mu(\mu_r)\right]$ are computed as shown in Eq. (15).

$$E\left[\mu(\mu_r)\right] = \frac{\Delta\delta}{N_n} \sum_{\delta} \sum_{k=1.N_n} E\left[\frac{\gamma_k}{\delta}\right] \times p(\delta) \quad (15)$$

Every N_n neighbors of γ_k lies in $\left[\mu_r - \delta, \mu_r + \delta\right]$, after marginalizing over δ. Hence, the $N_n - 1$ neighbor is a mixture of $G'\left(\mu_f, \sigma^2, \mu_r - \delta, \mu_r + \delta\right)$ with p_f and $G'\left(\mu, \sigma^2, \mu_r - \delta, \mu_r + \delta\right)$ with p_r. The expected value of $\mu(\mu_r)$ is then calculated using Eq. (15). In order to compute the variance of $\mu(\mu_r)$, again marginalize the value δ and it is mathematically denoted in Eq. (16).

$$Var\left[\mu(\mu_r)\right] = \int_{-\infty}^{+\infty} \left(\mu - E\left[\mu\right]\right)^2 p(\mu)\, d\mu$$

$$= \int_{-\infty}^{+\infty} \left(\mu - E\left[\mu\right]\right)^2 \int_0^{+\infty} \left\{ p\left(\frac{\mu}{\delta}\right) p(\delta)\, d\delta \right\} d\mu$$

$$= \int_0^{+\infty} \left\{ \int_{-\infty}^{\infty} \left(\mu - E\left[\mu\right]\right)^2 p\left(\frac{\mu}{\delta}\right) d\mu \right\} p(\delta)\, d\delta \quad (16)$$

Restore the numerical integration once again by adding and subtracting $E\left[\mu/\delta\right]$, as represented in Eq. (17).

$$Var\left[\mu(\mu_r)\right] \cong \Delta\delta \sum_{\delta} \sum_{k=1..N_n} \left\{ \frac{\mathrm{var}\left[\gamma_k/\delta\right]}{N_n^2} + \left(E\left[\gamma_k/\delta\right] - E\left[\mu\right]\right)^2 \right\} . p(\delta) \quad (17)$$

As an alternative to NN methodology, collect the neighbor's square distance from the reference patch. The SNN patch $\{\gamma_k\}, k = 1,..N_n$ is minimized using Eq. (18).

$$\left| d^2(\mu_r, \gamma_k) - o.2\sigma^2 \right|, o = 1 \quad (18)$$

Where, o is stated as additional offset parameter. Then, $Var\left[\mu(\mu_r)\right]$ and $E\left[\mu(\mu_r)\right]$ are computed for comparing the prediction error of SNN and NN. Finally, Fischer's approximation $\left(\sqrt{2x_p^2} \cong G\sqrt{2P-1}, 1\right)$ is applied in equation (1) for a single patch $P = 1$, where it is defined in equation (19).

$$d^2(\mu_r, \gamma) \cong \sigma \times \sqrt{2P-1} + G\left(0, \sigma^2\right) = \sigma + G\left(0, \sigma^2\right) \quad (19)$$

The SNN technique effectively diminishes the prediction error of the noise free patches with low signal to noise ratio. The developed SNN technique is not optimal for noisy images which contains small features of interest, because Gaussian noise prevents the determination of the correct coefficients for averaging that leads to over smoothing. To address this concern, WAT is included in SNN for smoothing the images. The output of SNN is indicated in figure 2, which is contaminated with sigma $\sigma = 5$. In this research, the experimental validation is done with various noise ranges (0, 0.1, 0.35, 0.65, 0.8, 0.9 and 1) and neural network neighbors are fixed as 361 and 16.

Figure 2. $\sigma = 5$, a) Noisy image, b) ground truth image, c) denoised image with noise range $SNN_{.0}^{16}$, d) denoised image with noise range $SNN_{.35}^{16}$ and e) denoised image with noise range $SNN_{.8}^{16}$

C. Wave Atom Transform

Usually, the transforms like WAT, contourlets, steerable pyramid, complex wavelets and cortex transform are developed from multi-scale geometric analysis. Among these methods, WAT delivers better image representation that includes many oscillatory patterns. WAT adapts local directions of the image patterns and represents the anisotropic patterns that are associated with the axes. Compared to other transforms, two new indexes are introduced in WAT for better understanding of the digital images. The index α represents whether the image decomposition is multi-scale $(\alpha=1)$ or not $(\alpha=0)$. In addition, the index β represents whether the image basic elements are poorly directional $(\beta=1)$ or fully directional $(\beta=0)$.The adaptive transform decomposes the digital images by localizing width $2^{-\alpha j}$ and the length $2^{-\beta j}$. In frequency domain, the WAT is determined by paving the co-ordinates of width $2^{-\alpha j}$ and the length $2^{-\beta j}$.Generally, the wavelets comprise of multi-resolution, directional and complex analysis, which corresponds to $\alpha=\beta=1$ .Though, in Gabor transform $(\alpha=0, and\ \beta=0)$, ridgelet transform $(\alpha=1, and\ \beta=0)$ and curvelet transform $(\alpha=1, and\ \beta=1/2)$. The WAT is characterized as a relation between multidirectional and multiscale aspects with $(\alpha=1/2, and\ \beta=1/2)$ [21-22].

Identifying the optimality of decomposition is equal to minimize the decomposition energy [23]. WAT is developed using the tensor products of adequately selected one dimensional wavelet packets and that is represented as $\psi_{m.n}^{j}(x)$, where $j,m>0$ and $n\in z$. Therefore, the one dimensional wavelet packets are centered around $X_{j,n}=2^{-j}n$ and $\mp\psi_{j,m}=\mp\pi 2^{j}m$ in frequency and space domains corresponding with $C_1 2^{j}<m<C_2 2^{j}$. Where, $C_1<C_2$ are stated as positive constants. In frequency domain, the basic function is achieved by translated version of ψ_m^0 and dyadic scaled that is mathematically denoted in Eq. (20).

$$\psi_{m,n}^{j}(x)=\psi_m^j\left(x-2^{j}n\right)-2^{j/2}\psi_m^0\left(2^{j}x-n\right) \tag{20}$$

Then, the subscript $d^2(\mu_r,\gamma)$ is included in Eq. (20) and the two dimensional orthonormal basis is mathematically indicated in the Eq. (21) and (22).

$$\varphi_{d^2(\mu_r,\gamma)}^{+}(x_1,x_2)=\psi_{m_1}^{j}\left(x_1-2^{-j}n_1\right)\psi_{m_2}^{j}\left(x_2-2^{-j}n_2\right) \tag{21}$$

$$\varphi_{d^2(\mu_r,\gamma)}^{-}(x_1,x_2)= H\psi_{m_1}^{j}\left(x_1-2^{-j}n_1\right)H\psi_{m2}^{j}\left(x_2-2^{-j}n_2\right) \tag{22}$$

Where, H is represented as Hilbert transformation value. By combining the Eq. (21) and (22) generates the wave atom tight frame as indicated in the Eq. (23) and (24).

$$\varphi_{d^2(\mu_r,\gamma)}^{(1)}=\frac{\varphi_{d^2(\mu_r,\gamma)}^{+}+\varphi_{d^2(\mu_r,\gamma)}^{-}}{2} \tag{23}$$

$$\varphi_{d^2(\mu_r,\gamma)}^{(2)}=\frac{\varphi_{d^2(\mu_r,\gamma)}^{+}-\varphi_{d^2(\mu_r,\gamma)}^{-}}{2} \tag{24}$$

In this scenario, WAT is used with directional frame for removing Gaussian noise in the digital images. After decomposing the images, hard thresholding T_H is applied to the coefficients, where the threshold is three times better than the value of standard deviation. Hard thresholding is defined in Eq. (25).

$$T_H=\begin{cases} x & for\,|x|\geq t \\ 0 & in\,all\,other\,regions \end{cases} \tag{25}$$

Where, t is indicated as threshold value. A plot of T_H is graphically indicated in figure 3.

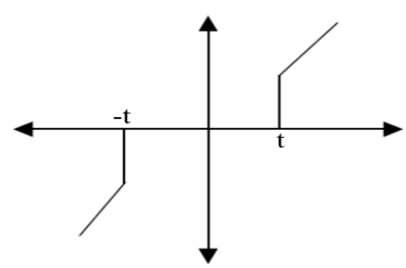

Figure 3. Plot of hard thresholding T_H

Meanwhile, the step by step procedure of SNN-WAT is given below,

Step 1: At first, the Right Circular Shift (RCS) process is employed in the digital images for noise removal, which is the output of SNN technique.

Step 2: Once the RSC process is accomplished, then two dimensional WAT is applied. Where the wave atom coefficients are achieved by using two dimensional WAT.

Step 3: Then, hard thresholding is used to threshold the value of wave atom coefficients.

Step 4: Inverse two dimensional WAT is applied to obtain the step 3 results.

Step 5: Lastly, left circular shift process is applied to get of the step 4 results and it marks the completion of denoising procedure. The experimental analysis about the proposed model is indicated below.

4. Experimental results

In this segment, the simulation outcome of the SNN-WAT model is validated with dissimilar performance metrics. In this scenario, MATLAB (2018a) environment was used with 128 GB RAM, i7 processor and two TB hard disc for experimental validation. Here, the proposed SNN-WAT model performance is compared with NLM-SNN [19], FFDNet [26], ADNet [27], and ADNet-B [27] for validating the effectiveness of the proposed model. Additionally, the quantitative analysis of SNN-WAT is done by varying $\sigma\epsilon\ [5,10,15,20,25,35,40\ and\ 50]$ of Gaussian noise and evaluated by the performance metrics; PSNR, SSIM, MSSIM, FSIM, $FSIM_C$ [24], and GMSD [25]. In this study, the undertaken performance measures are utilized for comparing the performance of $k'(x,y)$ and $k(x,y)$. Hence, the higher PSNR indicates the best quality of denoised image, which is calculated using MSE value that is represented in Eq. (26),

$$MSE = \frac{1}{mn}\sum_{x=0}^{m-1}\sum_{y=0}^{n-1}\left\|k(x,y)-k'(x,y)\right\|^2 \qquad (26)$$

Where, noisy image is indicated as $k(x,y)$, denoised image is denoted as $k'(x,y)$ and the image dimensions are stated as $m\ and\ n$. The formula to calculate PSNR is given in Eq. (27).

$$PSNR = 20\log_{10}\left(\frac{\max\left(k(x,y)\right)}{\sqrt{MSE}}\right) \qquad (27)$$

Additionally, the proposed model effectiveness is investigated by using the performance metrics like SSIM and MSSIM, which are mathematically indicated in the Eq. (28) and (29).

$$SSIM(i,j) = \frac{\left(2\mu_i\mu_j + c_1\right)\left(2\sigma_{ij}+c_2\right)}{\left(\mu_{i^2}+\mu_{j^2}+c_1\right)\left(\sigma_{i^2}+\sigma_{j^2}+c_2\right)} \qquad (28)$$

$$MSSIM(k,k') = \frac{1}{W}\sum_{y=1}^{W}\left(SSIM(i,j)\right) \qquad (29)$$

where, w indicates windows in the denoised and noisy image, standard deviation and mean states $\sigma\ and\ \mu$ and $c_1\ and\ c_2$ indicates constant values.

A. Quantitative investigation

In this segment, KODAK dataset (a sample image) is undertaken for validating the performance of SNN-WAT and existing model with various noise ranges, sigma value and neural network neighbors is fixed as 361 and 16. In this study, the existing and proposed model performance is validated by means of PSNR, SSIM, MSSIM, FSIM, $FSIM_C$ and GMSD. Initially, the undertaken images are contaminated with Gaussian noise and then attempt has been performed for reconstructing the images with better visual quality. Gaussian noise is a wideband noise that arises during image acquisition, due to high temperature in electronic circuit and poor illumination. So, Gaussian noise is concentrated in this study compared to other noises and because it is applicable many computer vision and multimedia applications.

The contaminated images with sigma $\sigma = 5\ and\ 10$ are graphically represented in the figures 4 and 5, where 4(a) and 5(a) are noisy images and 4(b) and 5(b) are ground truth images (original images). The figures 4(c) and 5(c) represents the images after applying SNN-WAT model with noise range $SNN-WAT_{.0}^{16}$. The figures 4(d) and 5(d) states the images after applying SNN-WAT with noise range $SNN-WAT_{.35}^{16}$. In addition, figures 4(e) and 5(e) indicates the images after using SNN-WAT model with noise range $SNN-WAT_{.8}^{16}$.

(a) (b) (c) (d) (e)

Figure 4. $\sigma = 5$, a) Noisy, b) ground truth, c) denoised with noise range $SNN-WAT_{.0}^{16}$, d) denoised with noise range $SNN-WAT_{.35}^{16}$ and e) denoised with noise range $SNN-WAT_{.8}^{16}$

Figure 5. $\sigma = 10$,a) Noisy, b) ground truth, c) denoised with noise range $SNN - WAT_{.0}^{16}$, d) denoised with noise range $SNN - WAT_{.35}^{16}$ and e) denoised with noise range $SNN - WAT_{.8}^{16}$

TABLE II. PERFORMANCE INVESTIGATION OF THE EXISTING AND PROPOSED MODEL WITH $\sigma = 5$

$\sigma = 5$						
Methods	PSNR	SSIM	MSSIM	FSIM	$FSIM_C$	GMSD
$NLM - SNN_{.0}^{361}$ [19]	38.34	0.9851	0.9921	0.9941	0.9939	0.013
$NLM - SNN_{.0}^{16}$ [19]	38.08	0.9847	0.9919	0.9949	0.9947	0.0113
$NLM - SNN_{.1}^{16}$ [19]	38.08	0.9847	0.9919	0.9949	0.9947	0.0113
$NLM - SNN_{.35}^{16}$ [19]	38.08	0.9847	0.9919	0.9949	0.9947	0.0113
$NLM - SNN_{.65}^{16}$ [19]	38.14	0.985	0.992	0.9949	0.9947	0.0113
$NLM - SNN_{.8}^{16}$ [19]	38.23	0.9854	0.9922	0.9948	0.9946	0.0115
$NLM - SNN_{.9}^{16}$ [19]	38.28	0.9854	0.9923	0.9946	0.9945	0.0118
$NLM - SNN_{1.0}^{16}$ [19]	38.29	0.9852	0.9921	0.9944	0.9942	0.0124
$SNN - WAT_{.0}^{361}$	39.34	0.98874	0.99561	0.99413	0.99316	0.00733
$SNN - WAT_{.0}^{16}$	38.14	0.98374	0.99103	0.99443	0.99416	0.00743
$SNN - WAT_{.1}^{16}$	38.14	0.98374	0.99103	0.99443	0.99416	0.00743
$SNN - WAT_{.35}^{16}$	38.14	0.98374	0.99103	0.99443	0.99416	0.00743
$SNN - WAT_{.65}^{16}$	39.36	0.98881	0.99561	0.99421	0.99396	0.00791
$SNN - WAT_{.8}^{16}$	39.23	0.98228	0.99352	0.99183	0.99158	0.03608
$SNN - WAT_{.9}^{16}$	38.54	0.98994	0.99173	0.98821	0.98794	0.05435
$SNN - WAT_{1.0}^{16}$	39.06	0.98657	0.95952	0.98494	0.98457	0.06342

TABLE III. PERFORMANCE INVESTIGATION OF THE EXISTING AND PROPOSED MODEL WITH $\sigma = 10$

$\sigma = 10$						
Methods	PSNR	SSIM	MSSIM	FSIM	$FSIM_C$	GMSD
$NLM - SNN_{.0}^{361}$ [19]	34.84	0.9634	0.9804	0.9814	0.9811	0.0338
$NLM - SNN_{.0}^{16}$ [19]	33.96	0.958	0.9773	0.9861	0.9856	0.0269
$NLM - SNN_{.1}^{16}$ [19]	33.96	0.958	0.9773	0.9861	0.9856	0.0269
$NLM - SNN_{.35}^{16}$ [19]	33.96	0.958	0.9773	0.9861	0.9856	0.0269

$NLM-SNN_{.65}^{16}$ [19]	34.19	0.961	0.9789	0.9861	0.9857	0.0266
$NLM-SNN_{.8}^{16}$ [19]	34.51	0.9639	0.9805	0.9856	0.9852	0.0274
$NLM-SNN_{.9}^{16}$ [19]	34.66	0.9645	0.9809	0.9845	0.9841	0.0291
$NLM-SNN_{1.0}^{16}$ [19]	34.71	0.9635	0.9803	0.9828	0.9824	0.0319
$SNN-WAT_{.0}^{361}$	34.44	0.97639	0.98323	0.98929	0.99363	0.01912
$SNN-WAT_{.0}^{16}$	34.34	0.97385	0.98788	0.98897	0.98989	0.01863
$SNN-WAT_{.1}^{16}$	34.34	0.97385	0.98788	0.98897	0.98989	0.01863
$SNN-WAT_{.35}^{16}$	34.34	0.97385	0.96788	0.98897	0.98989	0.01863
$SNN-WAT_{.65}^{16}$	35.40	0.96865	0.98139	0.98471	0.98412	0.01977
$SNN-WAT_{.8}^{16}$	35.44	0.96889	0.98157	0.98439	0.98981	0.02040
$SNN-WAT_{.9}^{16}$	34.39	0.96875	0.98098	0.98283	0.98627	0.02649
$SNN-WAT_{1.0}^{16}$	34.89	0.96716	0.98830	0.98057	0.98997	0.03372

By analyzing tables II and III, the proposed SNN-WAT model attained significant denoising performance compared to existing model in light of PSNR, SSIM, MSSIM, FSIM, $FSIM_C$ and GMSD in all the noise ranges and $\sigma=(5, and\, 10)$ .In the case of $(0.65, \sigma=5)$, the proposed model delivered a maximum PSNR value of 39.36 dB. By validating tables II and III, the proposed model (SNN-WAT) attained better performance in image denoising related to existing model (NLM-SNN [19]) by means of PSNR, SSIM, MSSIM, FSIM, $FSIM_C$ and GMSD. In table III, the proposed model showed comparable performance in a rare cases $\left(NLM-SNN_{.0}^{361}\ and\ NLM-SNN_{.9}^{16}\right)$ of PSNR value, due to image pixel quality. But the content is retrieved properly by the proposed SNN-WAT model and showed better results in other performance measures.

Additionally, in the table IV and figure 6, the proposed model attained better performance in image denoising related to existing model (NLM-SNN [19]) in light of PSNR, SSIM, MSSIM, FSIM, $FSIM_c$ and GMSD in all the noise ranges and $\sigma=20$. The proposed model (SNN-WAT) achieved better performance in denoising, because it captures the pattern across oscillation and also the coherence of the pattern with the oscillations. While preserving the image edges, the proposed model considers local structural similarity for narrowing down the spatial window. Graphically, the contaminated images with sigma $\sigma=20$ is denoted in figure 6.

(a) (b) (c) (d) (e)

Figure 6. $\sigma=20$ a) Noisy, b) ground truth, c) denoised with noise range $SNN-WAT_{.0}^{16}$, d) denoised with noise range $SNN-WAT_{.35}^{16}$ and e) denoised with noise range $SNN-WAT_{.8}^{16}$

TABLE IV. PERFORMANCE INVESTIGATION OF THE EXISTING AND PROPOSED MODEL WITH $\sigma = 20$

$\sigma = 20$						
Methods	PSNR	SSIM	MSSIM	FSIM	$FSIM_C$	GMSD
$NLM - SNN_{.0}^{361}$ [19]	31.18	0.9109	0.9505	0.9475	0.9468	0.0749
$NLM - SNN_{.0}^{16}$ [19]	29.21	0.8802	0.9343	0.9646	0.9633	0.0607
$NLM - SNN_{.1}^{16}$ [19]	29.21	0.8802	0.9343	0.9646	0.9633	0.0607
$NLM - SNN_{.35}^{16}$ [19]	29.21	0.8802	0.9343	0.9646	0.9633	0.0607
$NLM - SNN_{.65}^{16}$ [19]	29.75	0.8948	0.942	0.9653	0.9641	0.0572
$NLM - SNN_{.8}^{16}$ [19]	30.45	0.9086	0.9493	0.9631	0.9621	0.0583
$NLM - SNN_{.9}^{16}$ [19]	30.81	0.9119	0.9511	0.9585	0.9576	0.0635
$NLM - SNN_{1.0}^{16}$ [19]	30.93	0.9084	0.949	0.951	0.9503	0.0719
$SNN - WAT_{.0}^{361}$	31.47	0.94387	0.92870	0.96897	0.96714	0.03932
$SNN - WAT_{0}^{16}$	31.47	0.94381	0.95879	0.96902	0.97730	0.03937
$SNN - WAT_{.1}^{16}$	31.47	0.94381	0.95879	0.96902	0.97730	0.03937
$SNN - WAT_{.35}^{16}$	31.47	0.94381	0.95879	0.96902	0.97730	0.03937
$SNN - WAT_{.65}^{16}$	31.62	0.94509	0.94943	0.97589	0.97473	0.04163
$SNN - WAT_{.8}^{16}$	31.62	0.94535	0.96921	0.97353	0.97252	0.04539
$SNN - WAT_{.9}^{16}$	31.60	0.94542	0.95907	0.97236	0.97146	0.04766
$SNN - WAT_{1.0}^{16}$	31.47	0.94477	0.94801	0.97829	0.97744	0.05268

(a) (b) (c) (d) (e)

Figure 7. $\sigma = 40$ a) Noisy, b) ground truth, c) denoised with noise range $SNN - WAT_{.0}^{16}$, d) denoised with noise range $SNN - WAT_{.35}^{16}$ and e) denoised with noise range $SNN - WAT_{.0}^{16}$

In figure 7 and table V, the performance investigation is carried-out for all the noise ranges and $\sigma = 40$ in light of PSNR, SSIM, MSSIM, FSIM, $FSIM_c$ and GMSD. The contaminated image with sigma $\sigma = 40$ is graphically denoted in figure 7, where 7(a) is a noisy image and 7(b) is a ground truth image. Figures 7(c), 7(d) and 7(e) represents the denoised image after applying SNN-WAT with the noise ranges $SNN - WAT_{.0}^{16}$, $SNN - WAT_{.35}^{16}$ and $SNN - WAT_{.8}^{16}$. By investigating table V, the proposed model (SNN-WAT) attained superior performance in denoising in light of PSNR, SSIM, MSSIM, FSIM, $FSIM_C$ and GMSD with $\sigma = 40$. In the proposed model, SNN technique reduces the prediction error of noise free image patches that deblur the lower contrast image details with minimum signal to noise ratio and system complexity for different Gaussian noise level [19].

In addition, KODAK dataset (24 images) are utilized to analyze the overall performance of SNN-WAT model and existing models; FFDNet [26], ADNet [27], and ADNet-B [27] in light of PSNR value. In this scenario, the performance analysis is done for different noise ranges (0, 0.1, 0.35, 0.65, 0.8. 0.9, and 1), $\sigma = (15, 25, 35, \text{and } 50)$ and neural network neighbors is fixed as 361 and 16. By inspecting table VI, the proposed SNN-WAT model attained better performance in image denoising compared to the existing models by means of PSNR value. In this scenario, WAT technique effectively captures the coherence of the pattern along with the oscillations that improves the smoothing of image edge details. As stated in the literature section, the combined SNN-WAT model overcomes the problems such as over smoothing and ill posed denoising issue [26-27]. In table VII, the overall comparison between the proposed and the existing models is presented. Hence, the maximum obtained PSNR, SSIM, MSE, and SNR value is given in table VII.

TABLE V. PERFORMANCE INVESTIGATION OF THE EXISTING AND PROPOSED MODEL WITH $\sigma = 40$

$\sigma = 40$						
Methods	PSNR	SSIM	MSSIM	FSIM	$FSIM_C$	GMSD
$NLM-SNN^{361}_{.0}$ [19]	27.71	0.8184	0.8893	0.8856	0.8844	0.1303
$NLM-SNN^{16}_{.0}$ [19]	25.38	0.7522	0.8591	0.9237	0.9206	0.1061
$NLM-SNN^{16}_{.1}$ [19]	25.38	0.7522	0.8591	0.9237	0.9206	0.1061
$NLM-SNN^{16}_{.35}$ [19]	25.38	0.7522	0.8591	0.9237	0.9206	0.1061
$NLM-SNN^{16}_{.65}$ [19]	25.38	0.7522	0.8591	0.9237	0.9206	0.1061
$NLM-SNN^{16}_{.8}$ [19]	25.38	0.7522	0.8591	0.9237	0.9206	0.1061
$NLM-SNN^{16}_{.9}$ [19]	25.49	0.758	0.8624	0.9243	0.9213	0.1043
$NLM-SNN^{16}_{1.0}$ [19]	26.38	0.7942	0.8813	0.9248	0.9223	0.0977
$SNN-WAT^{361}_{.0}$	29.32	0.92345	0.87392	0.93441	0.94012	0.07274
$SNN-WAT^{16}_{.0}$	29.20	0.91089	0.87695	0.93281	0.93017	0.07454
$SNN-WAT^{16}_{.1}$	29.20	0.91089	0.87695	0.93281	0.93017	0.07454
$SNN-WAT^{16}_{.35}$	29.20	0.91089	0.87695	0.93281	0.93017	0.07454
$SNN-WAT^{16}_{.65}$	29.10	0.91186	0.87637	0.93099	0.93893	0.07871
$SNN-WAT^{16}_{.8}$	30.06	0.91283	0.87675	0.93982	0.92890	0.07969
$SNN-WAT^{16}_{.9}$	29.03	0.91456	0.87779	0.92730	0.92564	0.08354
$SNN-WAT^{16}_{1.0}$	28.92	0.91376	0.87681	0.92085	0.92944	0.09382

Table VI. Overall performance of SNN-WAT model and existing models by means of PSNR value

PSNR value				
Methods	$\sigma = 15$	$\sigma = 25$	$\sigma = 35$	$\sigma = 50$
FFDNet [26]	34.55	32.11	30.56	28.99
ADNet [27]	34.76	32.26	30.68	29.10
ADNet-B [27]	34.53	32.03	30.44	28.81
$SNN-WAT^{361}_{.0}$	34.89	33.97	31.09	30.92
$SNN-WAT^{16}_{.0}$	34.87	34.43	31.82	30.07
$SNN-WAT^{16}_{.1}$	34.90	34.43	30.98	30.02
$SNN-WAT^{16}_{.35}$	34.98	34	32	29.67
$SNN-WAT^{16}_{.65}$	35.08	34.26	32.08	29.77
$SNN-WAT^{16}_{.8}$	35.12	34.90	31.92	29.56
$SNN-WAT^{16}_{.9}$	34.98	33.81	31.44	29.19
$SNN-WAT^{16}_{1.0}$	35.69	33.95	31.84	29.94

TABLE VII. .OVERALL COMPARISON BETWEEN THE PROPOSED AND THE EXISTING MODELS

Authors	PSNR (dB)	SSIM	MSE	SNR
L. Fan et al. [11]	27.45	0.788	-	-
Y. Zhang et al. [12]	26.36	-	-	23.38
G. Wang et al. [13]	28.35	-	258.09	-
H. R. Shahdoosti, and S. M. Hazavei, [16]	30.26	0.809	-	-
B. Jin, et al [18]	28.67	-	-	-
SNN-WAT	**32.57**	**0.931**	**189**	**28.02**

5. CONCLUSION

In this research article, a hybrid model is presented for image denoising, which is the combination of SNN and WAT. The importance of the proposed model is to restore the digital images without a previous knowledge of the spectral density of the ground truth or original image. In this research work, the proposed model performance is validated on KODAK dataset, where the images are contaminated with Gaussian noise of sigma $\sigma \epsilon [5, 10, 15, 20, 25, 35, 40 \text{ } and \text{ } 50]$ and noise range of (0, 0.1, 0.35, 0.65, 0.8. 0.9, and 1.0). In the experimental section, the proposed model performance is investigated by means of PSNR, SSIM, MSSIM, FSIM, $FSIM_C$ and GMSD. In image denoising, the proposed model averagely enhanced maximum of 4 dB and minimum of 0.1 dB of PSNR value compared to NLM-SNN, FFDNet, ADNet and ADNet-B techniques. In future work, a modified filtering technique can be included in the proposed model to further enhance the denoising performance in the digital images.

REFERENCES

[1] P.D. Swami, and A. Jain, “Image denoising by supervised adaptive fusion of decomposed images restored using wave atom, curvelet and wavelet transform,” Signal, Image and Video Processing, vol. 8, pp. 443-459, 2014.

[2] A. Phophalia, and S. K. Mitra, "Rough set based bilateral filter design for denoising brain MR images," Appl. Soft Comput., vol. 33, pp. 1-14, 2015.

[3] Q. Wang, J. Ma, S.Yu, and L. Tan, "Noise detection and image denoising based on fractional calculus," Chaos, Solitons Fractals, vol. 131, pp. 109463, 2020.

[4] Z. Lyu, C. Zhang, and M. Han, "A nonsubsampled countourlet transform based CNN for real image denoising," Signal Process. Image Commun., vol. 82, pp. 115727, 2020.

[5] A. Bal, M. Banerjee, P. Sharma, and M. Maitra, "An efficient wavelet and curvelet-based PET image denoising technique," Med. Biol. Eng. Comput., vol. 57, pp. 2567-2598, 2019.

[6] F.P. An, and X.W. Zhou, "Adaptive image denoising based on support vector machine and wavelet description," Opt. Rev., vol. 24, pp. 660-667, 2017.

[7] H. Naimi, A. B. H. Adamou-Mitiche, and L. Mitiche, "Medical image denoising using dual tree complex thresholding wavelet transform and Wiener filter," Journal of King Saud University-Computer and Information Sciences, vol. 27, pp. 40-45, 2015.

[8] M. H. Alkinani, and M. R. El-Sakka, "Patch-based models and algorithms for image denoising: a comparative review between patch-based images denoising methods for additive noise reduction," EURASIP Journal on Image and Video Processing, vol. 2017, pp. 1-27, 2017.

[9] G. Chen, P. Zhang, Y. Wu, D. Shen, and P. T. Yap, "Denoising magnetic resonance images using collaborative non-local means," Neurocomputing, vol. 177, pp. 215-227, 2016.

[10] A. Asokan, and J. Anitha, "Adaptive Cuckoo Search based optimal bilateral filtering for denoising of satellite images," ISA Trans., 2019.

[11] L. Fan, X. Li, H. Fan, and C. Zhang, "An adaptive boosting procedure for low-rank based image denoising," Signal Process., 2019.

[12] Y. Zhang, S. Xu, K. Chen, Z. Liu, and C.P. Chen, "Fuzzy density weight-based support vector regression for image denoising," Information Sciences, vol. 339, pp. 175-188, 2016.

[13] G. Wang, H. Zhu, and Y. Wang, "Fuzzy decision filter for color images denoising," Optik, vol. 126, pp. 2428-2432, 2015.

[14] J. J. J. Babu, and G. F. Sudha, "Adaptive speckle reduction in ultrasound images using fuzzy logic on Coefficient of Variation," Biomed. Signal Process. Control, vol. 23, pp. 93-103, 2016.

[15] V. P. Ananthi, and P. Balasubramaniam, "A new image denoising method using interval-valued intuitionistic fuzzy sets for the removal of impulse noise," Signal Process., vol. 121, pp. 81-93, 2016.

[16] H. R. Shahdoosti, and S. M. Hazavei, "A new compressive sensing based image denoising method using block-matching and sparse representations over learned dictionaries," Multimedia Tools and Applications, vol. 78, pp. 12561-12582, 2019.

[17] M. Rakhshanfar, and M. A. Amer, "Efficient cascading of multi-domain image Gaussian noise filters," Journal of Real-Time Image Processing, pp. 1-13, 2019.

[18] B. Jin, S. J. You, and N. I. Cho, "Bilateral image denoising in the Laplacian subbands," EURASIP Journal on Image and Video Processing, vol. 2015, pp.26, 2015.

[19] I. Frosio, and J. Kautz, "Statistical nearest neighbors for image denoising," IEEE Trans. Image Process., vol. 28, pp. 723-738, 2018.

[20] X. Li, J. Xiao, Y. Zhou, Y. Ye, N. Lv, X. Wang, S. Wang, and S. Gao, "Detail retaining convolutional neural network for image denoising," J. Visual Commun. Image Represent., pp. 102774, 2020.

[21] J. Rajeesh, R. S. Moni, and S. S. Kumar, "Performance analysis of wave atom transform in texture classification," Signal, Image and Video Processing, vol. 8, pp. 923-930, 2014.

[22] Z. Haddad, A. Beghdadi, A. Serir, and A. Mokraoui, "Image quality assessment based on wave atoms transform," IEEE International Conference on Image Processing, pp. 305-308, 2010.

[23] Z. Mbarki, H. Seddik, and E. B. Braiek, "A rapid hybrid algorithm for image restoration combining parametric Wiener filtering and wave atom transform," J. Visual Commun. Image Represent., vol. 2016, pp. 694-707.

[24] L. Zhang, L. Zhang, X. Mou,and D. Zhang, "FSIM: A feature similarity index for image quality assessment," IEEE Trans. Image Process., vol. 20, pp. 2378-2386, 2011.

[25] W. Xue, L. Zhang, X. Mou, and A. C. Bovik, "Gradient magnitude similarity deviation: A highly efficient perceptual image quality index," IEEE Trans. Image Process., vol. 23, pp. 684-695, 2013.

[26] K. Zhang, W. Zuo, and L. Zhang, "FFDNet: Toward a fast and flexible solution for CNN-based image denoising", IEEE Transactions on Image Processing, vol.27, no.9, pp.4608-4622, 2018.

[27] C. Tian, Y. Xu, Z. Li, W. Zuo, L. Fei, and H. Liu, "Attention-guided CNN for image denoising", Neural Networks, vol.124, pp.117-129, 2020.

Akula Suneetha received her B.Tech (CSE) from Sir C R Reddy College of Engineering, Andhra University in the year 2005 and M.Tech (CSE) Degree from Jawaharlal Nehru Technological University Hyderabad, Telangana, India in the year 2009 .She is currently pursuing Ph.D. Degree in Acharya Nagarjuna University. She is currently working as Assistant professor in the Department of CSE, KKR & KSR Institute of Technology & Sciences, Guntur, Andhra Pradesh affiliated to JNTUK University. Her research area is Fuzzy Image Processing. She is having 13 years of Teaching Experience.

Edara Srinivasa Reddy, Professor & Dean, University College of Engineering & Technology, Acharya Nagarjuna University, A.P. He did Philosophical Doctorate in Computer Science and Engineering from Acharya Nagarjuna University, Guntur. He did Master of Technology in Computer Science and Engineering from Sir MokhsagundamVisweswariah University, Bangalore. He also did Master of Science from Birla Institute of Technological Sciences, Pilani. He guided several research scholars of PhD. His research areas of interest are in various domains including Digital Image Processing. He has published 5 Books, 78 Journals and attended 45 Conferences and 24 Workshops.